Scale-up Design of Ultrasound Irradiator for Advanced Oxidation Process (AOP) Using COMSOL Simulation

Zongsu Wei [*1]
[1]The Ohio State University, Columbus, OH, USA

*Corresponding author: HI 470, 2070 Neil Avenue, Columbus, OH, 43210, USA; Phone: (614) 906-8511; Fax: (614) 292-3780; E-mail: wei.187@osu.edu

Abstract: In this paper, COMSOL Multiphysics was used as a tool to design and characterize an ultrasound irradiator with a multi-stepped configuration, which aims to overcome disadvantages of typical irradiators and to enhance contaminant removal in large-scale water treatments. In the simulation, three different physics were coupled together for each component of the designed ultrasonic system: piezoelectric material model for transducer, linear elastic material model for irradiator, and pressure acoustics model for reactor. The COMSOL adequately simulated the acoustic wave generation in the piezoelectric transducer and propagation through the irradiator. The simulated acoustic pressure level shows the multi-stepped irradiator successfully introduced multiple high pressure regions and thus more reactive zones. Acoustic simulations in the water tank suggested the designed irradiator has a great capacity for large-scale AOPs. These compatible simulation results to experimental measurements indicate COMSOL is a reliable tool in the design and characterization of a scaled-up ultrasound irradiator.

Keywords: Ultrasound, Irradiator, Piezoelectric, Cavitation, Advanced Oxidation Process (AOP)

1. Introduction

Ultrasound has been considered a promising green technology for the advanced oxidation process (AOP) since it adds no chemicals to the treated water. It has been shown to effectively destroy various organic and inorganic contaminants in water [1]. Ultrasound induces cavitation bubbles in the aqueous solution, and collapse of those bubbles generates localized "hot spots" where temperature and pressure are as high as 5000 K and 1000 atm, respectively [2]. In this extreme condition, thermolysis and •OH (from water molecule dissociation by heat) oxidation are two mechanisms for the contaminant degradation [1, 2].

Although ultrasound technology shows great potential in the AOP, the commonly-used ultrasound irradiator (e.g., horn type in Figure 1a) generates a localized cavitation and non-uniform cavitation field in treatment reactors. The inhomogeneous treatment makes it very challenging to scale-up the AOP with the typical irradiator [3]. Therefore, a novel configuration design of ultrasound irradiator is necessary to enhance and maximize the cavitation-induced chemical effects for large-scale AOP.

In the design process, computational simulation was commonly used as references. When expecting efficiency and economics in the design of an expensive large-scale system for AOP, the computational tool seems more attractive since it can easily investigate different reactor geometries, irradiator configurations, and ultrasound frequencies to optimize the design. Of those computational tools, COMSOL Multiphysics have been applied to simulate acoustic field and sonochemistry in reactors [4-6], which provided compatible results to laboratory measurements. The design and characterization become much simple and straightforward with the aid of computational simulations.

In this study, COMSOL simulation was carried out to assist an ultrasound irradiator design and characterization. A multi-stepped configuration (Figure 1b) was introduced to bring more energy-emitting surface and large cavitation volume. This "proof-of-concept" study with COMSOL simulation started with the simplest scenario, in which it was assumed that materials assigned including water and stainless steel were linear media. In addition, another assumption was made that acoustic waves were time-harmonic since sinusoidal alternating current (AC) was the power source.

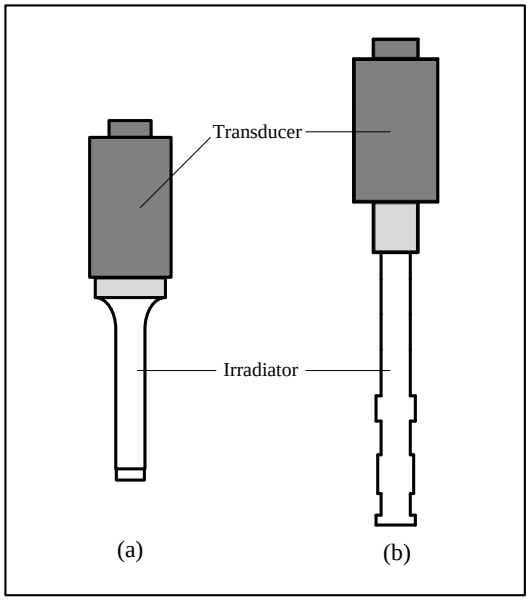

Figure 1. Configurations of a typical irradiator (a) and the designed irradiator (b).

2. Methodology

The simulation was established to 2D symmetric dimension due to the symmetric configuration of the scaled-up ultrasound system with a piezoelectric transducer, a newly designed irradiator (20 kHz, 26 – 38 mm in diameter, and 28.0 cm in length) and a water tank (610 mm × 610 mm × 450 mm in dimension and 167.5 L in volume). The ultrasonic system involves different physical phenomena [3, 7, 8]. The piezoelectric material in the transducer converts electrical energy to mechanical vibration which passes through the ultrasound irradiator and is intensified at the end of the irradiator. The irradiator emits those amplified mechanical waves (ultrasound waves) to water, and those waves then propagate in the water tank radially. Therefore, three different models were selected to simulate the ultrasonic system: piezoelectric material model for transducer, linear elastic material model for irradiator, and pressure acoustics model for water. Each model is governed by its own equations.

2.1 Piezoelectric Material Model

The piezoelectric effect is a phenomenon that an applied stress on piezoelectric materials induces electric polarization or an applied electric field induces dimension change for piezoelectric materials [3, 8-10]. In the transducer, the synthetic ceramics of PZT (lead zirconate titanate) provides an electrical field and a mechanical field at the same time. The electromechanical behaviors of the isotropic PZT can be expressed by two linearized constitutive equations [7, 9-11]:

$$Stress-charge \quad \begin{cases} \boldsymbol{T} = c_E \boldsymbol{S} - e^T \boldsymbol{E} \\ \boldsymbol{D} = e\boldsymbol{S} + \varepsilon_S \boldsymbol{E} \end{cases}$$

$$Strain-charge \quad \begin{cases} \boldsymbol{S} = s_E \boldsymbol{S} + d^T \boldsymbol{E} \\ \boldsymbol{D} = d\boldsymbol{T} + \varepsilon_T \boldsymbol{E} \end{cases}$$

where **T** is stress vector (6×1 matrix), **S** is strain vector (6×1 matrix), **E** is electric field intensity vector (3×1 matrix), **D** is electric flux density vector (3×1 matrix), c_E is elastic coefficients (6×6 matrix) at constant electric field strength, e^T is dielectric permittivity matrix (6×3), e is dielectric permittivity (3×6 matrix), ε_S is dielectric matrix (3×3) at constant mechanical strain, s_E is elastic compliance (6×6 matrix) in a constant electric field, d^T is piezoelectric strain constant matrix (6×3), d is piezoelectric strain constant (3×6 matrix), ε_T is dielectric matrix (3×3) at constant mechanical stress.

2.2 Linear Elastic Material Model

The particle displacements generated in the piezoelectric transducer are transmitted to the irradiator since they are connected to each other [7, 8]. Both PZT and stainless steel are isotropic and elastic materials. Therefore, their linear elastic behavior is governed by the Newton's Second Law [11, 12]:

$$-\rho\omega^2\boldsymbol{u} - \nabla \cdot \sigma = \mathbf{F}_V e^{i\phi}$$

where **u** is particle displacement, σ is stress, F_V is force per volume, and $e^{i\varphi}$ indicates the AC.

2.3 Pressure Acoustics Model

The pressure acoustics model has been used to simulate the ultrasound propagation in the water. The acoustic wave equation is given as follows [7, 8, 10-12]:

Table 1: Initial input for three domains

Liquid domain	Material	Water
	ρ	1000 kg/m^3
	c_S	1418 m/s
Irradiator domain	Material	1000 kg/m^3
	ρ	7850 kg/m^3
	E (Young's modulus)	205E09 Pa
	ν (Poisson's ratio)	0.28
Transducer domain	Material	PZT-5H
	ρ	7500 kg/m^3
	c_E (6×6 matrix)	$\begin{bmatrix} 1.27205E11 & 2.34742E10 & 2.29885E10 & & & \\ 2.34742E10 & 8.02122E10 & 2.29885E10 & & & \\ 2.29885E10 & 2.29885E10 & 1.27205E11 & & & \\ & & & 8.46702E10 & & \\ & & & & 8.46702E10 & \\ & & & & & 1.17436E11 \end{bmatrix}$ Pa
	e^T (6×3matrix)	$\begin{bmatrix} 0.00000 & 0.00000 & -6.62281 \\ 0.00000 & 0.00000 & -6.62281 \\ 0.00000 & 0.00000 & 23.2403 \\ 0.00000 & 17.0345 & 0.000000 \\ 0.00000 & 17.0345 & 0.000000 \\ 0.00000 & 0.00000 & 0.000000 \end{bmatrix}$ C/m^2
	ε_S (3×3 matrix)	$\begin{bmatrix} 1704.4 & & \\ & 1704.4 & \\ & & 1433.6 \end{bmatrix}$
	s_E (6×6 matrix)	$\begin{bmatrix} 1.65E-11 & 4.26E-11 & 4.35E-11 & & & \\ 4.26E-11 & -4.78E-12 & 4.35E-11 & & & \\ 4.35E-11 & 4.35E-11 & 1.65E-11 & & & \\ & & & -8.45E-12 & & \\ & & & & -8.45E-12 & \\ & & & & & 2.07E-11 \end{bmatrix}$ Pa
	d^T (6×3matrix)	$\begin{bmatrix} 0.00000 & 0.00000 & -2.74E-10 \\ 0.00000 & 0.00000 & -2.74E-10 \\ 0.00000 & 0.00000 & 5.93E-10 \\ 0.00000 & 7.41E-10 & 0.000000 \\ 0.00000 & 7.41E-10 & 0.000000 \\ 0.00000 & 0.00000 & 0.000000 \end{bmatrix}$ C/N
	ε_T (3×3 matrix)	$\begin{bmatrix} 3130 & & \\ & 3130 & \\ & & 3400 \end{bmatrix}$

$$\frac{1}{\rho c^2}\frac{\partial^2 p}{\partial t^2} + \nabla \cdot \left(\frac{1}{\rho}(\nabla \mathrm{p} - \mathbf{q})\right) = \boldsymbol{Q}$$

where p (Pa) is acoustic pressure, ρ (kg/m^3) is density of water, and c (m/s) is speed of ultrasound propagation in the water. The dipole source **q** (N/m^3) and the monopole source **Q** (1/s^2) are both optional. The combination ρc^2 is called the adiabatic bulk modulus (Pa).

Since ultrasound is longitudinal waves [13], there is no polarization (**q** = 0 and **Q** = 0) [14]. Water is assumed as an ideal liquid (ρ = constant and η = 0). Therefore, the wave equation for the acoustic pressure can be simplified to [7]:

$$\nabla^2 P - \frac{1}{c^2}\frac{\partial^2 P}{\partial t^2} = 0$$

This equation describes the acoustic pressure at any given point (x, y, z) and time t.

2.4 Boundary Condition and Initial Input

The setting of boundary conditions refers to COMSOL Modeling Guide and previous simulation studies [7, 8, 12, 15-17]. A structure-acoustic boundary was set to the interface between irradiator and water [8, 12]. Since ultrasound waves are longitudinal waves, the horn side was set as sound hard boundary at which the normal component of the acceleration is zero (there is no particle movements in the direction perpendicular to horn axis) [7]:

$$-\mathbf{n} \cdot \left(\frac{1}{\rho_0}(\nabla \mathrm{p} - \mathbf{q})\right) = 0$$

Displacements at the interface between water and wall of the tank was also considered as zero (u = 0 or P = 0) assuming the tank material with a large acoustic impedance sufficiently absorbed those coming acoustic waves. The particle displacement at the interface of transducer and irradiator was set to be equal [15-17]. Boundary conditions for surfaces contacting air were set to free (P = 0) [12].

The Initial value of electric potential was set to 110V, and default temperature was 293.15K. The liquid, transducer, and irradiator domains were assigned to linear water media, piezoelectric material (PZT-5H), and stainless steel material (AISI 4340), respectively. The input information of those three materials is summarized in Table 1.

3. Results and Discussion

First, in order to evaluate and compare the performance of our irradiator, the acoustic pressure level was calculated in COMSOL for both typical (Figure 2) and designed irradiators (Figure 3). The typical irradiator only delivers one high acoustic pressure area below its tip, whereas our multi-stepped design brings multiple high acoustic pressure regions around the "edges".

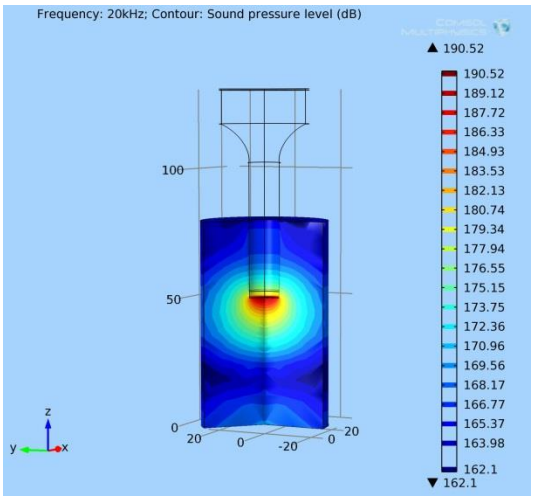

Figure 2. Scattered sound pressure level surrounding the typical irradiator (Unit for color label is dB).

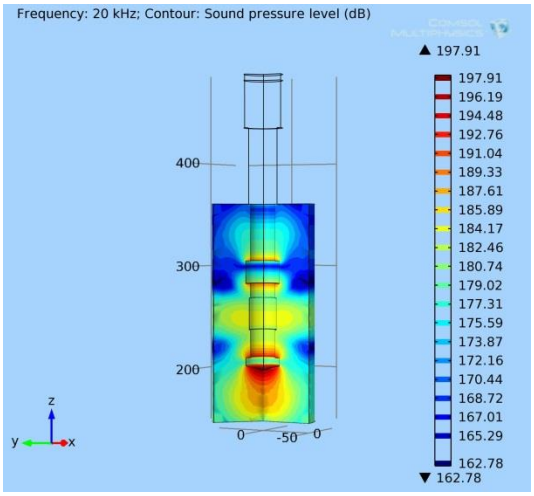

Figure 3. Scattered sound pressure level surrounding the designed irradiator (Unit for color label is dB).

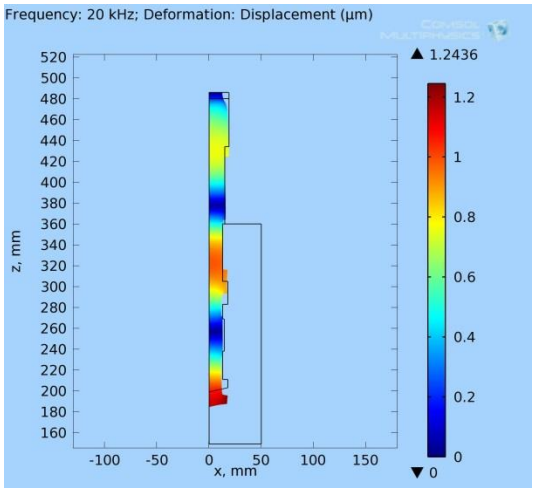

Figure 4. Deformation of transducer and irradiator (Unit for color label is μm).

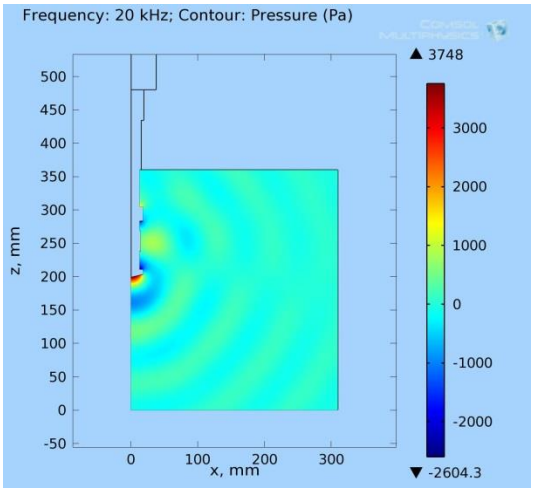

Figure 5. Simulation of acoustic pressure distribution in water tank in 2D (Unit for color label is Pa).

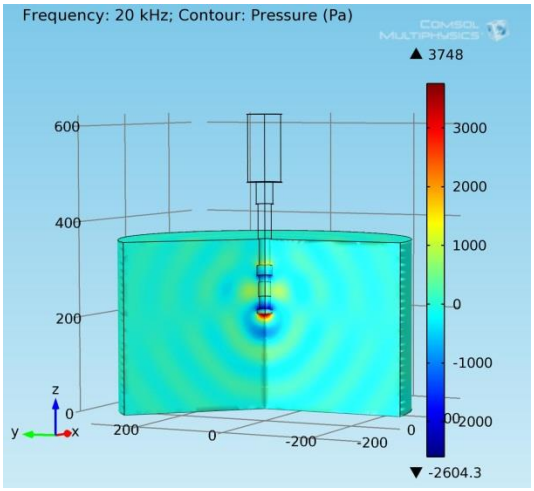

Figure 6. Simulation of acoustic pressure distribution in water tank in 3D (Unit for color label is Pa).

The simulation results are consistent with laboratory hydrophone measurements and sonochemiluminescence imaging [18]. Since a high acoustic pressure is the prerequisite for cavitation responsible for contaminant oxidation, the simulation results in Figure 3 demonstrate that the designed irradiator introduced more energy-emitting surfaces and therefore multiple reactive zones. For the other two domains besides water, the particle displacement (**u**) for the piezoelectric transducer and stainless steel irradiator is 1.24μm at maximum under the applied electrical and mechanical field, shown in Figure 4.

Next, the acoustic pressure distribution in the water tank was simulated to evaluate the large-scale application with designed irradiator, as shown in Figure 5 (2D) and Figure 6 (3D). In the simulated acoustic field, the red or yellow color along irradiator neck and below its tip also indicates a high acoustic pressure in those regions. At further regions, ultrasound waves propagate in the water forming ripple shapes. Acoustic attenuation is also observed by color changing from red to yellow, then to light yellow. The mapping of acoustic pressure in the water tank indicates the designed ultrasound irradiator with a large radiation radius (>20 cm) shows a great capacity for large-scale AOP.

4. Conclusion

The computed results have showed that the ultrasound irradiator design with a multi-stepped configuration improved cavitation effects as compared to typical irradiators generating localized cavitation. The COMSOL providing compatible results to experimental data seems to be a reliable and convenient tool for such scale-up design of ultrasound irradiator for AOP.

This simulation work applied the ideal condition for all physical models. For example, the simulation results may overestimate the particle displacements for both piezoelectric material and stainless steel irradiator since it is assumed there is no energy loss for piezoelectric effects and transmitting of mechanical energy from transducer to irradiator. The acoustic pressure distribution in the tank is symmetric and

linearly decreasing from center to edges due to the linearity of water media. Actually, the hydrophone measurements in the laboratory illustrate asymmetric and discrete distribution of acoustic pressure due to the acoustic cavitation, wave collision, and water movement by ultrasound irradiation.

Therefore, water viscosity, heat production, cavitation bubble, and model modification [8, 10, 19] will be added one by one to current simulation to obtain more reliable data in the future study. Even though this simplest simulation is not an accurate reflection of the real system, it is a worthy starting platform and valuable reference for future simulation design which can represent the real system setup.

5. References

1. Weavers, L.K., F.H. Ling, and M.R. Hoffmann, Aromatic compound degradation in water using a combination of sonolysis and ozonolysis, *Environmental Science & Technology*, **32**(18), 2727-2733 (1998).
2. Suslick, K.S., The chemical effects of ultrasound, *Scientific American*, **0**, 80-86 (1989).
3. Mason, J.M. and A. Tiehm, Advances in sonochemistry, **Vol. 6**, Connecticut: Jai Press (2001).
4. Csoka, L., S.N. Katekhaye, and P.R. Gogate, Comparison of cavitational activity in different configurations of sonochemical reactors using model reaction supported with theoretical simulations, *Chemical Engineering Journal*, **178**, 384-390 (2011).
5. Klima, J., A. Frias-Ferrer, J. Gonzalez-Garcia, J. Ludvik, V. Saez, and J. Iniesta, Optimisation of 20 kHz sonoreactor geometry on the basis of numerical simulation of local ultrasonic intensity and qualitative comparison with experimental results, *Ultrasonics Sonochemistry*, **14**(1), 19-28 (2007).
6. Trujillo, F.J. and K. Knoerzer, A computational modeling approach of the jet-like acoustic streaming and heat generation induced by low frequency high power ultrasonic horn reactors, *Ultrasonics Sonochemistry*, **18**(6), 1263-1273 (2011).
7. Xie, Y., Model analysis and experiment of sonochemical cell, Master Thesis, National Cheng Kung University (2008).
8. Yao, M., Analysis and experiment of resonant sonochemical cell, Master Thesis, National Cheng Kung University (2009).
9. Ikeda, T., Fundamentals of piezoelectricity, Oxford, UK: Oxford University Press (1996).
10. Nygren, M.W., Finite element modeling of piezoelectric ultrasonic transducers, in Department of Electronics and Telecommunications, Master Thesis, Norwegian University of Science and Technology (2011).
11. COMSOL, COMSOL Multiphysics user's guide, version 4.2 (2012).
12. COMSOL, COMSOL Multiphycis modeling guide, version 4.2 (2012).
13. Kinsler, L.E., A.R. Frey, A.B. Coppens, and J.V. Sanders, Fundamentals of acoustics, fourth edition, New York, NY: John Wiley & Sons (2000).
14. Mason, T.J. and J.P. Lorimer, Applied sonochemistry: The use of power ultrasound in chemistry and processing, Verlag GmbH, Weinheim: Wiley-VCH (2002).
15. Fu, Z.Q., X.J. Xian, S.Y. Lin, C.H. Wang, W.X. Hu, and G.Z. Li, Investigations of the barbell ultrasonic transducer operated in the full-wave vibrational mode, *Ultrasonics*, **52**(5), 578-586 (2012).
16. Lin, Z., Theory and design of ultrasonic horn, Beijing: Science Press (1987).
17. Peshkovsky, S.L. and A.S. Peshkovsky, Matching a transducer to water at cavitation: Acoustic horn design principles, *Ultrasonics Sonochemistry*, **14**, 313-322 (2007).
18. Wei, Z., R. Xiao, M. Cai, and L.K. Weavers, Designing and characterizing a multi-stepped ultrasonic horn for enhanced acoustic cavitation, *Ultrasonics Sonochemistry* (to be submitted).
19. Vogler, E.T. and C.V. Chrysikopoulos, Experimental investigation of acoustically enhanced solute transport in porous media, *Geophysical Research Letters*, **29**(15), 1-4 (2002).